Pyrazolato Metal Complexes – Synthesis, Characterization, and X-ray Crystal Structures of Heterotrimetallic Re–M_2 Derivatives (M = Cu, Ag, Au)

G.Attilio Ardizzoia,*[a][+] Girolamo La Monica,[a][+] Angelo Maspero,[a] Norberto Masciocchi,[b][+] and Massimo Moret*[b]

Keywords: Pyrazolato ligands / Rhenium / Group-11 metals / Heterometallic complexes

By treating $[(CO)_3Re(Hpz)_2(pz)]$ (Hpz = pyrazole) with $[Cu(CH_3CN)_4]BF_4$, $AgNO_3$, or [Au(tht)Cl] (tht = tetrahydrothiophene) in acetonitrile in the presence of Et_3N, the corresponding trinuclear complexes $\{(CO)_3Re(pz)_3[M(CH_3CN)]_2\}$ (**1a–c**) have been obtained. Treatment of complexes **1a–c** with cyclohexyl isocyanide (*c*-$C_6H_{11}NC$) afforded the derivatives $\{(CO)_3Re(pz)_3[M(c\text{-}C_6H_{11}NC)]_2\}$ (**2a–c**). Complexes **2a–c** have been characterized in solution by ^{1}H-NMR spectroscopy and in the solid state by single-crystal X-ray diffraction analysis.

Introduction

The synthesis of di- and polynuclear complexes bearing ligands that hold the metal centers in close proximity is an important objective in metal coordination chemistry. Interest in such systems arises mainly because of their potential role in multi-metal-centered catalysis, both in biological and industrial reactions.[1] The major effort in this field is to find convenient binucleating ligands capable of producing the desired activities. Deprotonated pyrazoles (pyrazolate anions) represent a significant class of binucleating ligands because of their ability to coordinate in an *exo*-bidentate fashion.[2][3]

We have recently described the synthesis and structural properties of the mononuclear bis(pyrazole)pyrazolate complex of rhenium(I), $[(CO)_3Re(Hpz)_2(pz)]$ (Hpz = pyrazole).[4] This species belongs to a limited class of complexes that, from a coordination point of view, are comparable to protonated tris(pyrazolyl)borate molecules.[5] The other reported members of this class, $[(\eta^5\text{-}C_5Me_5)Ir(Hpz)(pz)_2]$,[6] $[(\eta^6\text{-}p\text{-cymene})Ru(Hpz)(pz)_2]$,[7] and $[(\eta^6\text{-mesitylene})Ru(Hpz)(pz)_2]$,[8] when deprotonated to give the anionic species $[(\eta^5\text{-}C_5Me_5)Ir(pz)_3]^-$, $[(\eta^6\text{-}p\text{-cymene})Ru(pz)_3]^-$, and $[(\eta^6\text{-mesitylene})Ru(pz)_3]^-$, have been shown to behave, in some respects, akin to the tris(pyrazolyl)borate anion, acting as organometallic ligands toward a variety of metal ions.[8][9]

We report herein on the reactivity of $[(CO)_3Re(Hpz)_2(pz)]$ towards Group-11 metal ions and show that, in the presence of an appropriate deprotonating agent, this complex gives rise to the formally dianionic species $[(CO)_3Re(pz)_3]^{2-}$, which is capable of coordinating two different metal centers through the lone pairs of its three monodentate pyrazolate groups. This leads to trimetallic species of general formula $[(CO)_3Re(pz)_3(ML)_2]$ [M = Cu^I, Ag^I, Au^I; L = CH_3CN, *c*-$C_6H_{11}NC$].

Results and Discussion

Reactions of $[(CO)_3Re(Hpz)_2(pz)]$ with $[Cu(CH_3CN)_4]BF_4$, $AgNO_3$, and [Au(tht)Cl] (tht = tetrahydrothiophene) in acetonitrile in the presence of Et_3N led to the formation of trimetallic species formulated as $\{(CO)_3Re(pz)_3[M(CH_3CN)]_2\}$ [M = Cu (**1a**), Ag (**1b**), Au (**1c**)] (Equation 1).

$$[(CO)_3Re(Hpz)_2(pz)] + 2\ ML_nX \xrightarrow[-Et_3NHX,\ -\ n\ L]{Et_3N\ /\ CH_3CN} [(CO)_3Re(pz)_3\{M(CH_3CN)\}_2] \qquad [1]$$

*(ML_nX = [Cu(CH$_3$CN)$_4$]BF$_4$, AgNO$_3$ or [Au(tht)Cl], for **1a-c**, respectively)*

The very low thermal stability of complexes **1a–c**, leading to loss of coordinated CH_3CN ligands and the formation of decomposition by-products, hampered any further characterization of these species. However, when reaction according to Equation 1 was carried out in the presence of stoichiometric amounts of *c*-$C_6H_{11}NC$, the readily characterizable species $\{(CO)_3Re(pz)_3[M(c\text{-}C_6H_{11}NC)]_2\}$ [M = Cu (**2a**), Ag (**2b**), Au (**2c**)] were obtained.

The IR spectra of all three species feature three strong ν(CO) bands in the 2000–1800 cm^{-1} region, typical for a *fac* stereochemistry at the rhenium center[10] and reminiscent of the spectrum of the starting rhenium complex $[Re(CO)_3(Hpz)_2(pz)]$. The positions of these absorptions are only marginally affected by the nature of the Group-11 metal (see Table 1). Moreover, no absorption attributable to the N–H stretching was detected, confirming the presence, in species **2**, of the $[(CO)_3Re(pz)_3]^{2-}$ core.

The pattern of the IR bands in the ν(NC) region merits further comment. While the copper (**2a**) and the silver (**2b**) derivatives show two absorptions (2210, 2164 and 2225, 2192 cm^{-1}, respectively), suggesting similar structures for

[a] Dipartimento di Chimica Inorganica, Metallorganica e Analitica, Università di Milano e Centro CNR,
Via Venezian, 21, I-20133 Milano, Italy
E-mail: attilio@csmtbo.mi.cnr.it
[b] Dipartimento di Chimica Strutturale e Stereochimica Inorganica, Università di Milano e Centro CNR,
Via Venezian, 21, I-20133 Milano, Italy
[+] On leave from: Dipartimento di Scienze Chimiche, Fisiche e Matematiche, Università dell'Insubria, Via Lucini, 3, I-22100 Como, Italy

  1434–1948/99/0808–1301 $ 17.50+.50/0

Table 1. Characteristic IR frequencies [cm^{-1}] for complexes **2a**−**c** (Nujol mulls)

Complex	ν(CO)	ν(NC)
2a	2002, 1885, 1868	2210, 2164
2b	1999, 1882, 1860	2225, 2192
2c	2002, 1884, 1860	2253

both complexes, marked differences are observed for the gold derivative **2c**. Indeed, this species shows only one ν(NC) stretching at 2253 cm^{-1}, suggesting a structure distinct from that of the copper and silver derivatives.

As far as complexes **2a** and **2b** are concerned, taking into account that three pyrazolato groups (elemental analyses) and three CO molecules (IR) complete the coordination sphere about the rhenium center, the presence of two cyclohexyl isocyanide ligands bound to two copper (or silver) centers in different coordinative environments can be inferred. Given the ability of silver and copper to sustain digonal and trigonal geometries, it can be presumed that both such stereochemistries are present in the heterometallic species **2a** and **2b**. Under this assumption, the ν(NC) absorption at lower energy (2164 cm^{-1} for **2a**; 2192 cm^{-1} for **2b**) can be attributed to the cyclohexyl isocyanide group coordinated to the (more electron-rich) trigonal Cu^{I} and Ag^{I} centers.

The different situation found in complex **2c** can be rationalized by taking into account the strong tendency of gold(I) to maintain a linear digonal coordination geometry; indeed, the presence in **2c** of two Au^{I} centers bonded to one pyrazolate nitrogen atom and one cyclohexyl isocyanide ligand each is consistent with the observation of a single ν(NC) absorption.

The proposed stuctures of **2a**−**c** (Scheme 1) have been unequivocally confirmed by single-crystal X-ray diffraction studies.

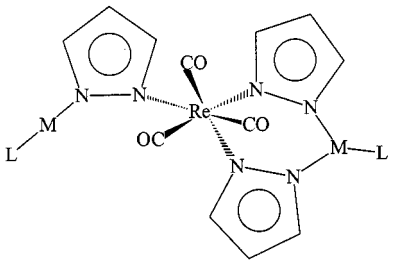

M = Ag, Cu L = c-$C_6H_{11}NC$

(A)

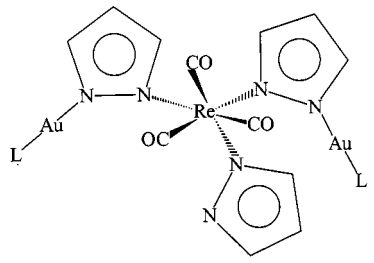

L = c-$C_6H_{11}NC$

(B)

Scheme 1. Schematic drawing of the connectivity patterns for complexes **2a**−**2b** (a) and **2c** (b)

Crystal Structures of 2a, 2b, and 2c

Crystals of compounds **2a**−**2c** are built up from neutral heterotrimetallic molecules held together by van der Waals interactions (see below for a more detailed description of the intermolecular interactions in **2c**). Figures 1−3 show ORTEP views of the molecular conformations of each compound, as observed in the solid state. Salient geometrical parameters are summarized in Table 2.

All three complexes contain an octahedral Re^{I} center bearing three carbonyl groups in a *fac* arrangement and three pyrazolato ligands able to connect to a second metal ion in an *exo*-bidentate mode. In **2a** and **2b**, two pyrazolate ligands are linked to the same Group-11 metal center M(1) [Cu(1) and Ag(1) for **2a** and **2b**, respectively] resulting in an Re−[N−N]$_2$−M(I) six-membered ring in the typical boat conformation. The difference in the ionic radii of the Cu^{I} and Ag^{I} species is mainly reflected in the M−N(2) and M−N(4) distances, which are about 0.25 Å longer in the Ag derivative. This leads to a remarkable narrowing of the

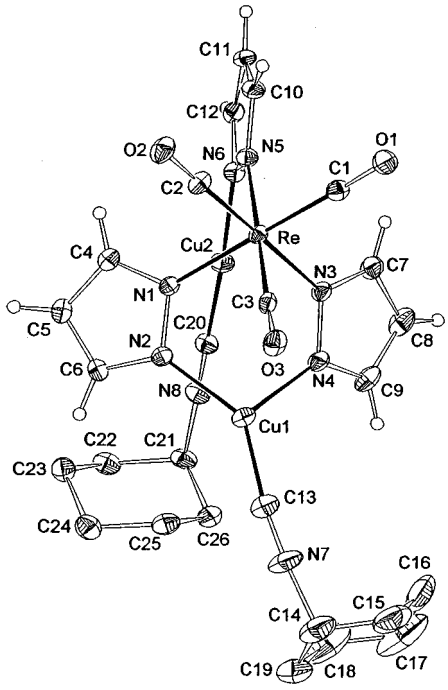

Figure 1. ORTEP drawing of complex **2a**, with partial labelling scheme; thermal ellipsoids are drawn at a 30% probability level; hydrogen atoms were given arbitrary radii

N(2)−M−N(4) angle in **2b** (see Table 2). The Cu^{I} [or Ag^{I}] center is further coordinated by a cyclohexyl isocyanide ligand, and therefore attains a planar-trigonal coordination environment [deviations from the coordination plane

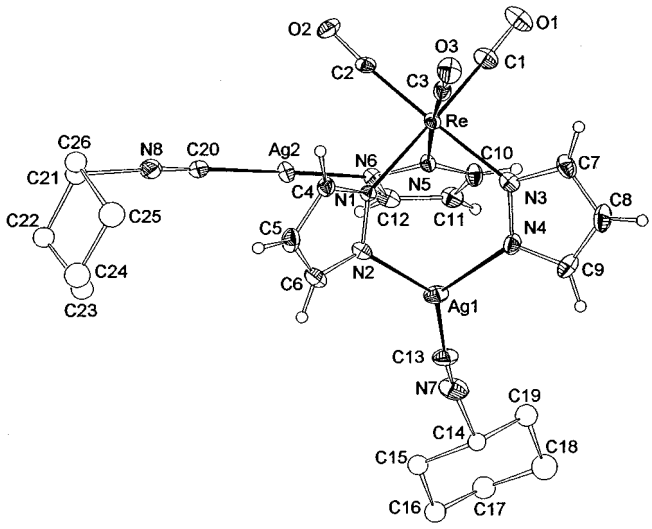

Figure 2. ORTEP drawing of complex **2b**, with partial labelling scheme; thermal ellipsoids are drawn at a 30% probability level; only the major component of the disordered cyclohexyl rings is drawn; hydrogen atoms were given arbitrary radii

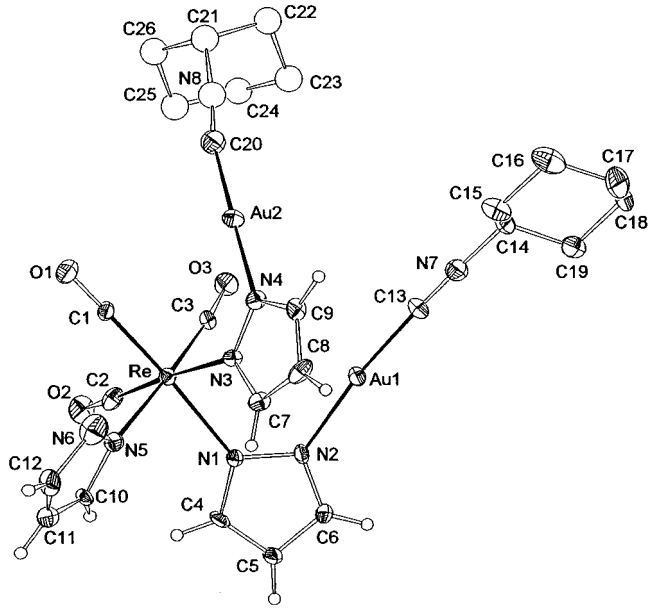

Figure 3. ORTEP drawing of complex **2c**, with partial labelling scheme; thermal ellipsoids are drawn at a 30% probability level; only the major component of the disordered cyclohexyl rings is drawn; hydrogen atoms were given arbitrary radii

amount to 0.084(4) and 0.016(4) Å for Cu(1) and Ag(1), respectively].

The remaining pyrazolate ligand is connected to the second Cu (**2a**) [or Ag (**2b**)] atom, the digonal coordination sphere of which is completed by another cyclohexyl isocyanide ligand. In this way, both molecules **2a** and **2b** contain one linearly coordinated and one trigonal-planar Group-11 metal ion, as was presumed on the basis of spectroscopic data. Nevertheless, the conformations of the Cu and Ag derivatives differ markedly in the solid state. Indeed, in **2a**, the Cu(1)−Re−N(5)−N(6) torsion angle is −0.2(5)° and

Table 2. Selected bond lengths [Å] and angles [°] for **2a−c** with e.s.d.′s in parentheses

Compound M	**2a** Cu	**2b** Ag	**2c** Au
Re−C(1)	1.902(8)	1.884(8)	1.891(11)
Re−C(2)	1.898(7)	1.919(8)	1.920(12)
Re−C(3)	1.903(8)	1.892(7)	1.886(11)
Re−N(1)	2.173(5)	2.199(5)	2.205(8)
Re−N(3)	2.181(5)	2.147(6)	2.189(8)
Re−N(5)	2.178(5)	2.170(5)	2.168(8)
M(1)−C(13)	1.828(8)	2.035(8)	1.920(11)
M(1)−N(2)	1.960(5)	2.218(5)	1.992(8)
M(1)−N(4)	1.986(6)	2.269(6)	
M(2)−N(4)			2.010(9)
M(2)−C(20)	1.834(7)	2.025(8)	1.946(14)
M(2)−N(6)	1.881(5)	2.096(5)	
O(1)−C(1)	1.151(8)	1.182(8)	1.161(11)
O(2)−C(2)	1.160(8)	1.138(7)	1.136(12)
O(3)−C(3)	1.162(8)	1.160(7)	1.163(11)
C(13)−M(1)−N(2)	139.7(3)	139.7(3)	173.4(5)
C(13)−M(1)−N(4)	117.7(3)	128.4(3)	
N(2)−M(1)−N(4)	102.0(2)	91.9(2)	
C(20)−M(2)−N(4)			176.9(4)
C(20)−M(2)−N(6)	169.3(3)	175.8(3)	
O(1)−C(1)−Re	178.3(7)	179.1(7)	178.4(10)
O(2)−C(2)−Re	177.8(6)	175.7(6)	176.7(11)
O(3)−C(3)−Re	177.0(6)	178.3(7)	173.3(10)

thus Cu(2) is nearly symmetrically buried within the pz(1−2) and pz(3−4) ligands, with an idealized mirror plane passing through Cu(1), Cu(2), Re, N(5), and N(6). On the contrary, the Ag(2)−CNC_6H_{11} moiety in **2b** is almost orthogonal to the Re−Ag(1) hinge [Ag(1)−Re−N(5)−N(6) 94.3(5)°]. Moreover, in terms of their "apparent" ionic radii, the Cu and Ag centers are about 0.1 Å larger in the trigonal than in the digonal environment.

In spite of the fact that all three complexes have the same general formula, the gold derivative **2c** has a completely different arrangement of the pyrazolate ligands. Owing to the lower tendency of gold for tricoordination, we observe a solid-state conformation with two digonally coordinated gold atoms, each bearing an isocyanide ligand and one nitrogen atom of a pyrazolato ligand. Thus, the third pyrazolato ligand is terminally bonded only to the rhenium atom in a monodentate fashion, leaving the second nitrogen lone pair unused.

While molecules **2a** and **2b** do not show significantly short intermolecular contacts in the crystals (which we have frequently observed for a number of Cu and Ag diazolato systems[11]), the packing of molecules **2c** reveals some additional features that merit further comment. Indeed, the crystal structure of **2c** reveals intermolecular interactions involving the gold atoms: Au(2)···Au(2)′ interactions of ca. 3.27 Å [relating molecules (x, y, z) and ($1-x$, $-y$, $-z$)] generate "dimeric" supramolecular entities; if the much looser Au(1)···Au(1)″ interactions [ca. 3.60 Å, relating (x, y, z) and ($-x$, $-y$, $-z$) molecules] are taken into account, an infinite 1-D concatenation of dimers can be envisaged, with pseudo-hexagonally packed chains of molecules running parallel to the a axis.

Solution Behaviour of 2a, 2b, and 2c

The structural analogies between complexes **2a** and **2b** found in the solid state were also seen in solution. The ^{1}H-NMR spectrum of **2b** recorded in CD_2Cl_2 at 303 K shows, beside the signals attributable to the cyclohexyl rings of the *c*-$C_6H_{11}NC$ ligands, a triplet centered at $\delta = 6.22$ ($J = 1.83$ Hz) attributable to C(4)−H of the pyrazolato rings, and two doublets ($\delta = 7.51$ and $\delta = 7.43$) attributable to C(3)−H and C(5)−H (Figure 4a). The observation of only one set of signals for each pyrazolato proton indicates that dynamic processes are operative that render all the pyrazolato groups present in the heterometallic species indistinguishable.

On lowering the temperature to 173 K, the ^{1}H-NMR spectrum of **2b** exhibits six signals at $\delta = 6.14$, 6.22, 7.07, 7.28, 7.45, and 8.03 in a 2:1:2:1:2:1 ratio, clearly attributable to C(4)−H (the two upfield signals) and C(3,5)−H of distinct pyrazolato groups (in a 2:1 ratio) (Figure 4c). Thus, although a partial broadening of the signals is still evident at this temperature, the observed pattern is consistent with the solid-state structure, indicating the almost complete freezing of the aforementioned dynamic process. At intermediate temperatures, the situation is less clear: The signals attributable to the protons in the 3- and 5-positions of the pyrazolate ligands collapse into a single resonance centered at $\delta = 7.41$ (Figure 4b). These features are seen over the 203−243 K range (with an increasing broadening of the signals); above 243 K, splitting into the two resonances observed at room temperature occurs.

An interpretation of the fluxional behaviour based on a concerted mutual exchange between the trigonal and digonal silver centers (as depicted in Scheme 2) can explain the limiting spectra at low and high exchange rates,[12] but is not able to account for the equivalence of the six protons in the 3- and 5-positions of the pyrazolate rings detected at intermediate exchange rates.

The spectroscopic observations may be rationalized by assuming that the exchange between the trigonal and digonal silver centers shown in Scheme 2 passes through transient intermediate species (species B_i in Scheme 3, $i = 1-3$) containing two singly bridged and one monodentate pyrazolato, as found in the solid state for the gold(I) derivative **2c**.

In fact, two exchange processes may be operative: one relating to the equilibrium between the doubly bridged and singly bridged species, $A_i - B_i$ (Scheme 3), and the second, responsible for rendering the 3- and 5-positions of the pyrazolate rings indistinguishable, involving N(1)/N(2) scrambling ($B_i - B'_i$), which is frequently found in complexes containing anionic monodentate pyrazolate ligands.[13] Hence, the ^{1}H-NMR pattern can be attributed to the relative rates of these two processes. Schematically, we can write the equilibrium as shown in Equation 2.

In the intermediate temperature range, the lifetime of the species B_i is sufficiently long to permit "hopping" of the metal atom between the two nitrogen atoms of the monodentate pyrazolate ring, making the 3- and 5-protons indis-

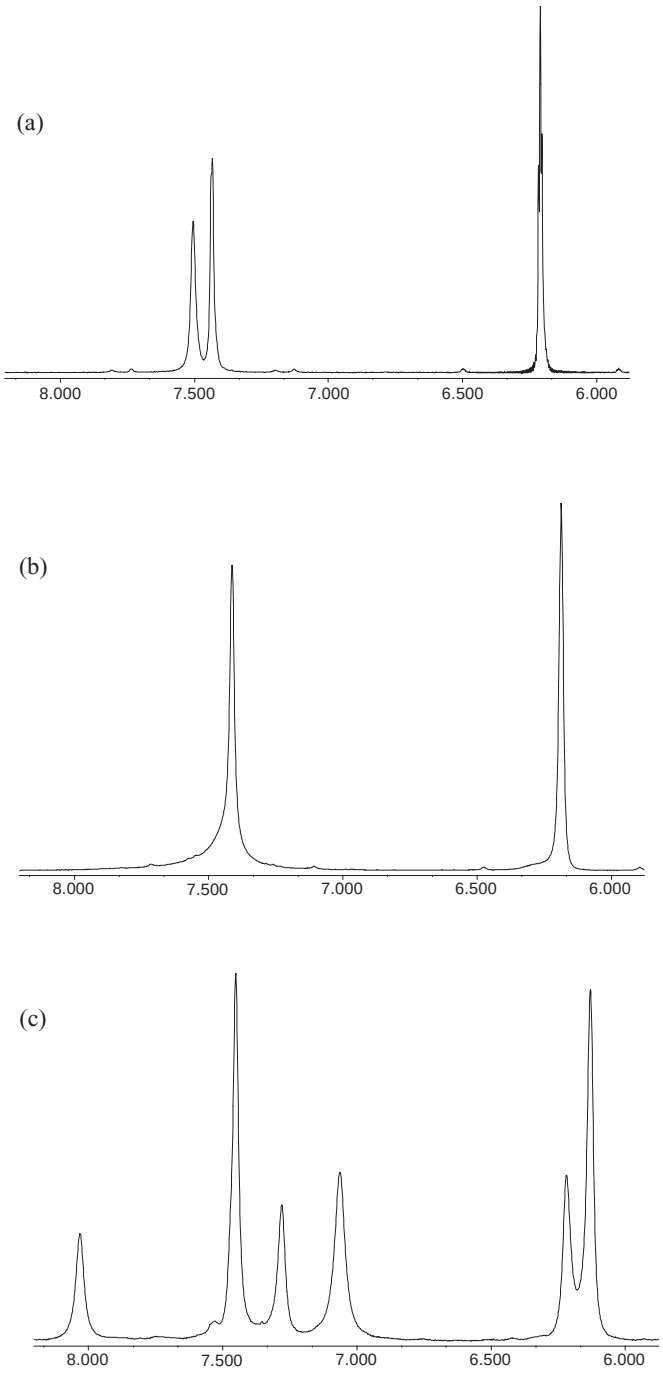

Figure 4. ^{1}H-NMR spectra (CD_2Cl_2 solution) in the pyrazolate-H region for compound **2b**: (a) at room temp., (b) at 213 K, and (c) at 173 K

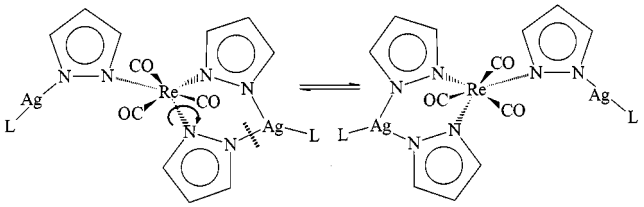

Scheme 2. Concerted mutual exchange between the trigonal and digonal silver centers in complex **2b**

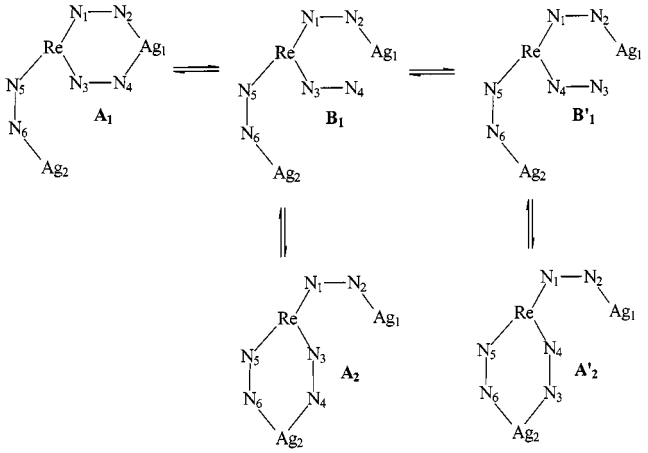

Scheme 3. Proposed mechanism for the dynamic process involving complex **2b**; similar equilibria are seen for all A_j species (see text)

$$A_i \rightleftharpoons \{B_i, B'_i\} \rightleftharpoons A_j \qquad [2]$$

tinguishable. At higher temperatures, the rapid opening/closure of the Ag−[N−N]$_2$−Ag metallocycle hampers this scrambling and hence the equilibration of the 3- and 5-positions. In terms of kinetic parameters (Arrhenius law), this corresponds qualitatively to rather different temperature dependences for the two processes, i.e. $\Delta E^{\neq}_{\text{open-close}} > \Delta E^{\neq}_{\text{scramble}}$ and $\ln A_{\text{open-close}} > \ln A_{\text{scramble}}$.

The room-temperature ^{1}H-NMR spectrum of the copper derivative **2a** closely matches that of species **2b** [two doublets centered at δ = 7.50 and 7.45, respectively; J = 1.92 Hz; a pseudo triplet at δ = 6.23]. On lowering the temperature to 173 K, all signals are broadened, but the overall spectral features do not change significantly. Indeed, the ^{1}H-NMR spectra of complex **2a** over the entire 303−173 K range are similar to those of **2b** in the "high" temperature range (above 243 K). This fact, assuming that the same fluxional processes active in **2b** also occur in **2a**, seems to indicate lower rigidity of the copper derivative compared to its silver counterpart.

As far as complex **2c** is concerned, the room-temperature ^{1}H-NMR spectrum shows, in the region of the pyrazole sig-

Table 3. Summary of single-crystal X-ray data and structure refinement parameters

Compound	**2a**	**2b**	**2c**
Empirical formula	$C_{26}H_{31}Cu_2N_8O_3Re$	$C_{26}H_{31}Ag_2N_8O_3Re$	$C_{26}H_{31}Au_2N_8O_3Re$
Molecular mass	816.87	905.53	1083.72
Crystal system	monoclinic	triclinic	monoclinic
Space group	$P2_1/c$	$P-1$	$P2_1/c$
a [Å]	18.631(6)	9.686(1)	13.521(1)
b [Å]	10.124(3)	13.344(1)	11.215(1)
c [Å]	16.660(7)	13.527(4)	21.016(1)
α [°]		109.43(1)	
β [°]	102.59(3)	100.70(1)	104.67(1)
γ [°]		102.24(1)	
V [Å^3]	3066.9(19)	1547.9(5)	3083.1(3)
Z	4	2	4
F(000)	1600	872	2000
D(calcd.) [g cm^{-3}]	1.769	1.943	2.335
Temperature [K]	293(2)	293(2)	293(2)
Diffractometer	CAD4	SMART	SMART
Radiation [Å]	0.71073	0.71073	0.71073
Absorption coefficient [mm^{-1}]	5.352	5.193	13.451
Crystal size [mm]	0.05 × 0.25 × 0.25	0.12 × 0.12 × 0.20	0.03 × 0.03 × 0.10
Scan method	ω	ω	ω
Scan interval [°]	1.5 + 0.35tanθ	0.3[a]	0.3[a]
Max time per refln. [s]	75	30[a]	60[a]
θ range [°]	3.0−25.0	2.2−28.5	2.0−28.0
Index ranges	$-22 \le h \le 21$	$-8 \le h \le 12$	$-13 \le h \le 16$
	$0 \le k \le 12$	$-17 \le k \le 17$	$-14 \le k \le 14$
	$0 \le l \le 19$	$-17 \le l \le 11$	$-25 \le l \le 26$
Reflections collected	5349	9774	16706
Independent reflections	5349 (R_{int} = 0.00)	7141 (R_{int} = 0.030)	6451 (R_{int} = 0.056)
Crystal decay	7%	none	none
Absorption correction	Ψ-scan	Sadabs	Sadabs
Min. transmission factor	0.44	0.695	0.742
Observed reflection criterion		all reflections	
Refinement method		full-matrix least squares on F_o^2	
Data/restraints/parameters	5349/0/361	7141/48/351	6451/15/326
Goodness-of-fit[b] on F_o^2	1.006	0.778	0.957
$R1$, $wR2$ indices[c] [$F_o > 4\sigma(F_o)$]	0.0305, 0.0691	0.0383, 0.0738	0.0492, 0.0724
$R1$, $wR2$ indices (all data)	0.0864, 0.0823	0.0772, 0.0817	0.1090, 0.0850
Largest diff. peak and hole [eÅ^{-3}]	1.214, −0.987	1.248, −1.386	1.023, −1.036
Weighting scheme:[d] a, b	0.0418, 2.5380	0.0333, 0	0.0306, 0

[a] Frame width and exposure time per frame. − [b] GoF = $[\Sigma w(F_o^2 - F_c^2)^2/(n-p)]^{1/2}$ where n is the number of reflections and p is the number of refined parameters. − [c] $R1 = \Sigma||F_o| - |F_c||/\Sigma|F_o|$, $wR2 = [\Sigma w(F_o^2 - F_c^2)/\Sigma wF_o^4]^{1/2}$. − [d] $w = 1/[\sigma(F_o^2) + (aP)^2 + bP]$ where $P = (F_o^2 + 2F_c^2)/3$.

nals, three doublets (6 H, in a 1:1:1 ratio) centered at δ = 7.77 (J = 1.92 Hz), δ = 7.53 (J = 1.75 Hz), and δ = 7.43 (J = 1.75 Hz), respectively, along with two triplets (3 H, in a 1:2 ratio) centered at δ = 6.25 and δ = 6.21, respectively. On lowering the temperature, the second doublet and the downfield triplet broaden and disappear, and finally, at −40°C, only three signals remain. Further lowering of the temperature leads to a drastic change in the spectrum with the appearance of new, partially overlapped signals. Presently, we are unable to give a complete explanation of this behaviour. This effect might be a manifestation of exchange processes similar to those observed for **2b**, but the non-equivalence of the Re−[N−N]$_2$−Au fragments further increases the complexity of the spectrum.

Conclusions

We have demonstrated herein that the organometallic complex [(CO)$_3$Re(Hpz)$_2$(pz)], once deprotonated, can act as a multidentate ligand towards a variety of metal atoms. The analogy with the tris(pyrazolyl)borate anion is, however, partially obscured by the fact that "tripod-like" coordination of Group-11 metal atoms was not observed, probably because of the specific electronic/steric requirements of the present systems, which favour low coordination numbers. Preliminary studies of Re−Mn derivatives have revealed that triply bridged [(CO)$_3$Re(μ-pz)$_3$MnL$_n$] systems can indeed be prepared, but these will be reported in a forthcoming paper.

Additionally, variable-temperature NMR analyses have clearly revealed the nonrigidity of the isolated species and have indicated that fluxionality can be attributed to simultaneous scrambling of monodentate pyrazolato ligands and ring-opening/closure equilibria, leading to a rather complex "argentotropic" behaviour.[12]

Experimental Section

General: Solvents were dried and purified by standard methods. Pyrazole (Aldrich Chemical Co.) was used as supplied. − Infrared spectra were recorded with a Bio Rad FT-IR 7 instrument. − ^{1}H-NMR spectra were acquired with a Bruker AC-300 FT spectrometer operating at 300.13 MHz. − Elemental analyses were performed at the Microanalytical Laboratory of this university (C, H, N). − All reactions were carried out under dry nitrogen using standard Schlenk techniques.

{(CO)$_3$Re(μ-pz)$_3$[Cu(CyNC)]$_2$} (2a): [(CO)$_3$Re(Hpz)$_2$(pz)][4] (150 mg, 0.317 mmol) was dissolved in acetonitrile (10 mL) and solid [Cu(CH$_3$CN)$_4$](BF$_4$)[14] (210 mg, 0.668 mmol) was added under stirring. Triethylamine (0.5 mL) was then added and the yellow solution was stirred for a further 15 min. A solution of cyclohexyl isocyanide (90 μL) in degassed CH_2Cl_2 (ca. 2 mL) was then added, leading to a colorless solution. After stirring for 30 min, the solvent was completely evaporated, the residue was treated with ethanol, and the white solid was collected by filtration, washed with ethanol, and dried in vacuo (155 mg, 60% yield). − $C_{26}H_{31}Cu_2N_8O_3Re$ (816.87): calcd. C 38.23, H 3.83, N 13.73; found C 38.06, H 3.78, N 13.38. − Crystals suitable for X-ray structure analysis were obtained by slow diffusion of *n*-hexane into dichloromethane solutions of the complex.

{(CO)$_3$Re(μ-pz)$_3$[Ag(CyNC)]$_2$} (2b): To a solution of [(CO)$_3$Re(Hpz)$_2$(pz)] (100 mg, 0.21 mmol) in acetonitrile (4 mL), was added a solution of $AgNO_3$ (94 mg, 0.55 mmol) in water (ca. 2 mL). Triethylamine (0.5 mL) was then added dropwise to the colorless solution, resulting in the sudden deposition of a white solid. The suspension was stirred for a further 15 min, and then the solid was collected by filtration, washed with water, and dried in vacuo (compound **1b**). **1b** was suspended in CH_2Cl_2 (ca. 2 mL) and cyclohexyl isocyanide (60 μL) was added to the white suspension, giving a colorless solution. The solvent was then evaporated in vacuo and the residue was treated with Et_2O, filtered, and dried in vacuo (108 mg, 57% yield). − $C_{26}H_{31}Ag_2N_8O_3Re$ (905.53): calcd. C 34.51, H 3.46, N 12.39; found C 34.83, H 3.54, N 12.35. − Crystals suitable for X-ray structure analysis were obtained by slow diffusion of *n*-hexane into dichloromethane solutions of the complex.

{(CO)$_3$Re(μ-pz)$_3$[Au(CyNC)]$_2$} (2c): To a stirred solution of [(CO)$_3$Re(Hpz)$_2$(pz)] (200 mg, 0.422 mmol) in acetonitrile (ca. 6 mL) at 0°C under nitrogen, was added [Au(tht)Cl][15] (tht: tetrahydrothiophene) (269 mg, 0.883 mmol). Tributylamine (0.5 mL) was then added dropwise. After a few minutes, a white solid separated from the colorless solution. The suspension was kept at 0°C and stirred for a further 3 h. The white solid was then collected by filtration and dried in vacuo (compound **1c**). Cyclohexyl isocyanide (60 μL) was added to a suspension of **1c** in CH_2Cl_2 (ca. 3 mL), giving a colorless solution. This solution was then concentrated to dryness and the residue was treated with ethanol. The white solid obtained was filtered off, washed with ethanol, and dried in vacuo (261 mg, 57% yield). − $C_{26}H_{31}Au_2N_8O_3Re$ (1083.72): calcd. C 28.78, H 2.88, N 10.33; found C 28.81, H 2.80, N 10.26. − Crystals suitable for X-ray structure analysis were obtained by slow diffusion of *n*-hexane into dichloromethane solutions of the complex, with protection from light.

Crystallography:[16] Crystals of **2a−c** were studied by conventional single-crystal X-ray methods; an overview of the methodology used can be found in ref.[11b] Owing to disorder involving the cyclohexyl moieties in **2b** and **2c**, special procedures were adopted during the structure refinement. For **2b**, the cyclohexyl rings were each described by two models having 62/38% and 52/48% occupancy factors, respectively. In **2c**, only one cyclohexyl ring was found to be disordered (with a 54/46% ratio) but required, in order to achieve least-squares stability, a common (isotropic) atomic displacement parameter. Hydrogen atoms of the disordered groups were omitted from the structure factor calculations. A list of crystal data, refinement parameters, and final agreement factors is presented in Table 3.

Acknowledgments

This work was supported by the Ministero dell'Università e della Ricerca Scientifica e Tecnologica (MURST) and by the Italian Consiglio Nazionale delle Ricerche (CNR). The technical support of Mr. Gianni Mezza is also acknowledged.

[1] [1a] R. Poilblanc, *Inorg. Chim. Acta* **1982**, *62*, 75−89. − [1b] C. Tejel, J. M. Villoro, M. A. Ciriano, J. A. López, E. Eguizábal, F. J. Lahoz, V. I. Bakhmutov, L. A. Oro, *Organometallics* **1996**, *15*, 2967−2978.

[2] [2a] S. Trofimenko, *Chem. Rev.* **1972**, *72*, 497−509. − [2b] S. Trofimenko, *Prog. Inorg. Chem.* **1986**, *34*, 115−210. − [2c] G. La Monica, G. A. Ardizzoia, *Prog. Inorg. Chem.* **1997**, *46*, 151−238.

[3] A few *endo*-bidentate pyrazolate complexes have been structurally characterized: [3a] C. W. Eigenbrot, Jr., K. N. Raymond, *Inorg. Chem.* **1981**, *20,* 1553−1556. − [3b] C. W. Eigenbrot, Jr., K. N. Raymond, *Inorg. Chem.* **1982**, *21,* 2653−2660. − [3c] D. Röttger, G. Erker, M. Grehl, R. Frölich, *Organometallics* **1994**, *13*, 3897−3902. − [3d] I. A. Guzei, G. A. Baboul, G. P. A. Yap, A. L. Rheingold, H. B. Schegel, C. H. Winter, *J. Am. Chem. Soc.* **1997**, *119*, 3387−3388. − [3e] J. E. Cosgriff, G. B. Deacon, *Angew. Chem.* **1998**, *110*, 298−299; *Angew. Chem. Int. Ed. Engl.* **1998**, *37*, 286−287 and references therein. − [3f] D. Pfeiffer, M. J. Heeg, C. H. Winter, *Angew. Chem.* **1998**, *110*, 2674−2676; *Angew. Chem. Int. Ed. Engl.* **1998**, *37,* 2517−2519.

[4] G. A. Ardizzoia, G. La Monica, A. Maspero, M. Moret, N. Masciocchi, *Eur. J. Inorg. Chem.* **1998**, 1503−1511

[5] S. Trofimenko, *Chem. Rev.* **1993**, *93*, 943−980.

[6] D. Carmona, L. A. Oro, M. P. Lamata, J. Elguero, M. C. Apreda, C. Foces-Foces, F. H. Cano, *Angew. Chem. Int. Ed. Engl.* **1986**, *25*, 1114−1115.

[7] D. Carmona, J. Ferrer, L. A. Oro, M. C. Apreda, C. Foces-Foces, F. H. Cano, J. Elguero, M. L. Jimeno, *J. Chem. Soc., Dalton Trans.* **1990**, 1463−1476.

[8] D. Carmona, F. J. Lahoz, R. Atencio, A. J. Edwards, L. A. Oro, M. P. Lamata, M. Esteban, S. Trofimenko, *Inorg. Chem.* **1996**, *35*, 2549−2557.

[9] [9a] D. Carmona, F. J. Lahoz, L. A. Oro, M. P. Lamata, S. Buzarra, *Organometallics* **1991**, *10*, 3123−3131. − [9b] D. Carmona, L. A. Oro, M. P. Lamata, M. L. Jimeno, J. Elguero, A. Belguise, P. Lux, *Inorg. Chem.* **1994**, *33*, 2196−2203. − [9c] D. Carmona, J. Ferrer, R. Atencio, F. Lahoz, L. A. Oro, M. P. Lamata, *Organometallics* **1995**, *14*, 2057−2065.

[10] R. J. Angelici, F. Basolo, A. J. Poe, *J. Am. Chem. Soc.* **1963**, *85*, 2215−2219.

[11] [11a] G. A. Ardizzoia, S. Cenini, G. La Monica, N. Masciocchi, A. Maspero, M. Moret, *Inorg. Chem.* **1998**, *37*, 4284−4292. − [11b] G. A. Ardizzoia, G. La Monica, A. Maspero, M. Moret, N. Masciocchi, *Inorg. Chem.* **1997**, *36*, 2321−2328. − [11c] N. Masciocchi, M. Moret, P. Cairati, A. Sironi, G. A. Ardizzoia, G. La Monica, *J. Chem. Soc., Dalton Trans.* **1995**, 1671−1675. − [11d] N. Masciocchi, M. Moret, P. Cairati, A. Sironi, G. A. Ardizzoia, G. La Monica, *J. Am. Chem. Soc.* **1994**, *116*, 7668−7676.

[12] This *argentotropism* has previously been reported for related species such as $\{(Cp^*)Ir(pz)_3[Ag(PPh_3)]_2\}^+$ and {(*p*-cymene)$Ru(pz)_3[Ag(PPh_3)]$}; see refs.[7,9b]

[13] [13a] A. L. Bandini, G. Banditelli, F. Bonati, G. Minghetti, F. Demartin, M. Manassero, *J. Organomet. Chem.* **1984**, *269*, 91−105. − [13b] D. Röttger, G. Erker, M. Grehl, R. Fröhlich, *Organometallics* **1994**, *13*, 3897−3902.

[14] G. J. Kubas, *Inorg. Synth.* **1979**, *19*, 90−91

[15] R. Uson, A. Laguna, M. Laguna, *Inorg. Synth.* **1989**, *26*, 85−86

[16] Crystallographic data for the structures reported in this paper have been deposited with the Cambridge Crystallographic Data Centre as supplementary publications nos. CCDC-112751 (**2a**), -112752 (**2b**), and -112753 (**2c**). Copies of the data can be obtained free of charge on application to CCDC, 12 Union Road, Cambridge CB2 1EZ, U.K. [Fax: (internat.) + 44-1223/336-033; E-mail: deposit@ccdc.cam.ac.uk].

Received December 30, 1998
[I98457]